CRYSTAL STRUCTURE AND MOLECULAR DOCKING STUDIES OF (*E*)-3-BENZO[*d*][1,3]DIOXOL-5-YL)-1-(3,4-DIMETHOXYPHENYL)PROP-2-EN-1-ONE

Submitted in partial fulfillment of the requirements for the award of
Master of Science in Chemistry

by

VIGNESH. K
(39910020)

DEPARTMENT OF CHEMISTRY
SCHOOL OF SCIENCE AND HUMANITIES

SATHYABAMA

INSTITUTE OF SCIENCE AND TECHNOLOGY
(DEEMED TO BE UNIVERSITY)
Accredited with Grade "A" by NAAC I 12B Status by UGC I Approved by AICTE
JEPPIAAR NAGAR, RAJIV GANDHI SALAI, CHENNAI - 600 119

APRIL – 2021

SATHYABAMA

INSTITUTE OF SCIENCE AND TECHNOLOGY
(DEEMED TO BE UNIVERSITY)
Accredited with "A" grade by NAAC I 12B Status by UGC I Approved by AICTE
Jeppiaar Nagar, Rajiv Gandhi Salai, Chennai – 600 119
www.sathyabama.ac.in

DEPARTMENT OF CHEMISTRY

BONAFIDE CERTIFICATE

This is to certify that this Project Report is the bonafide work of **VIGNESH.K (39910020)** who carried out the project entitled **"CRYSTAL STRUCTURE AND MOLECULAR DOCKING STUDIES OF (*E*)-3-(BENZO[*d*][1,3]DIOXOL-5-YL)-1-(3,4-DIMETHOXYPHENYL)PROP-2-EN-1-ONE"** under our Supervision from January 2021 to March 2021

Internal Guide	External Guide
Dr. J. KARTHIKEYAN	**Dr. M. MUTHU TAMIZH**

Head of the Department

Submitted for Viva voce Examination held on _____

Internal Examiner	External examiner

DECLARATION

I Mr. VIGNESH.K student of SATHYABAMA INSTITUTE OF SCIENCE AND TECHNOLOGY hereby declare that the Project Report entitled "CRYSTAL STRUCTURE AND MOLECULAR DOCKING STUDIES OF (*E*)-3-(BENZO[*d*][1,3]DIOXOL-5-YL)-1-(3,4-DIMETHOXYPHENYL)PROP-2-EN-1-ONE" one by me under the guidance of Dr. J Karthikeyan (Internal) and Dr. M. Muthu Tamizh Assistant Research Officer (Chemistry) (External), Siddha Central Research Institute, Chennai - 600106 is submitted in partial fulfillment of the requirements for the award of Master of Science degree in Chemistry.

DATE: **(VIGNESH K)**

PLACE: **SIGNATURE OF THE CANDIDATE**

ACKNOWLEDGEMENT

I am pleased to acknowledge my sincere thanks to Board of Management of SATHYABAMA for their kind encouragement in doing this project and for completing it successfully. I am grateful to them.

I convey my thanks to the **Dean**, School of Science and Humanities **Dr. J. Karthikeyan,** HoD, Department of Chemistry for providing me necessary support and details at the right time during the progressive reviews.

I would like to express my sincere and deep sense of gratitude to my Project Guide **Dr. J. Karthikeyan** (Internal Guide) for his valuable guidance and **Dr. M. Muthu Tamizh** (External Guide), Siddha Central Research Institute, Chennai suggestions and constant encouragement paved way for the successful completion of my project work.

I convey my deepest gratitude to **Dr. G. Suresh,** SPM Centre for Molecular Informatics, Chennai for his valuable guidance and time for the successful completion of the project

I wish to express my thanks to all Teaching and Non-teaching staff members of the Department of Chemistry who were helpful in many ways for the completion of the project.

ABSTRCT

A new chalcone has been designed and synthesized by Claisen-Schmidt condensation reaction by reacting 3, 4 Dimethoxy acetophenone and pipernol in presence of base. The formation of the product was confirmed by UV-Visible, FT-IR, FT-Raman, HRMS, 1D NMR (^{1}H, ^{13}C and DEPT 135) spectroscopic methods. The crystals were grown by slow evaporation in ethanol – dichloromethane – water system and the three dimensional X-ray structure of the synthesized compound was obtained using single crystal XRD method. Absorption and Vibrational spectra were predicted using Density Functional Theory (DFT) and compared with experimental data. Molecular Docking were performed for anti-bacterial activity in this work.

TABLE OF CONTENTS

LIST OF FIGURES

LIST OF TABLES

ABBREVIATIONS

FT-IR	Fourier Transform Infrared
FT-RAMAN	Fourier Transform Raman
NMR	Nuclear Magnetic Resonance
ppm	Parts Per Million
HR-ESI-MS	High-Resolution Electrospray ionization-Mass Spectrometry
DFT	Density Functional Theory

NOTATIONS

°C	Degree Celsius
h	Hours
cm^{-1}	Reciprocal centimeter
λ	Wavelength
nm	Nanometer
^{1}H	Hydrogen isotope – 1
^{13}C	Carbon isotope – 13
J	Coupling constant
Hz	Hertz
MHz	Mega Hertz
δ	Chemical shift
s	Singlet
d	Doublet
dd	Doublet of doublet
Å	Angstrom

CHAPTER - 1

INTRODUCTION

Chalcones are aromatic ketone which forms the central core for the various important biological compounds. It has various biological activities such as antimicrobial, anticancer, anti-inflammatory, antitubercular and antioxidant, etc depending upon on the substitution on chalcones. Chalcones are α, β unsaturated ketone contains aromatic moiety on each or either side. They possess conjugated double bond and a completely delocalized π-electron system on the aromatic rings. They found in most of the edible plants and it serves as the precursor for the synthesis of flavonoids and isoflavonoids [1]. Structurally modified chalcones has proven that it was useful for the development of various medicinal agents; hence chalcones has become an area of interest in both research and academic. Currently, it was widely used for the treatment of various diseases like viral disorder, cardio vascular disease, food additives, and cosmetic formulation ingredients [2]. There are different methods for preparing the chalcones but the most common being was synthesis via Claisen-Schmidt Condensation reaction. The Claisen-Schmidt Condensation reaction was basically Aldol Condensation reaction between the aromatic aldehyde and ketone which leads to product. The general example of a Claisen-Schmidt reaction was the reaction between benzaldehydes with the acetophenones to form the chalcones [3]. In recent days, the use of traditional medicinal plants such as ginger, curcumin and piper nigrum has increased for various ailments. [4] Especially, piper nigrum has posses interesting pharmacological effects and it contains piperine [5]. Piperine and its analogues showed a wide range of biological activities such as antitumor activity, antioxidant activity, antiinflammatory activity, antimycobacterial activity, insecticidal activity, etc… [6] Piperine contains 1, 3-Benzodioxole moiety in its structure [7]. The piperonal has, 1, 3-Benzodioxole moiety, hence it was choosed for the synthesizes of new chalcone. Herein we report the synthesize of (*E*)-3-(benzo[*d*][1,3]dioxol-5-yl)-1-(3,4-dimethoxyphenyl)prop-2-en-1-one from piperonal and 3, 4 dimethoxy acetophenone via Claisen- Schmidt

condensation reaction in basic condition NaOH and the structure of synthesized compound were confirmed by an various spectroscopic techniques such as UV-Vis, FT-IR, FT-Raman, NMR, HR-ESI-MS and Single crystal XRD methods. The Molecular docking was performed for the synthesized chalcone with Main protease of SARS-CoV-2 to understand the receptor-ligand interaction.

CHAPTER-2

LITERATURE SURVEY

2.1 Design, synthesis and biological evaluation of novel chalcone derivatives as antitubulin agents.

Hui Zhang et al (2012) prepared a series of novel chalcone derivatives and tested their biological activities as potential inhibitors of tubulin. The synthesized compound was assayed for growth-inhibitory activity against MCF-7 and A549 cell lines *in vitro*. A specific compound showed a influence in antipro-liferative activity against MCF-7 and A549 cell lines with IC_{50} values of 0.03 and 0.95 μg/mL and exhibited the most potent tubulin inhibitory activity with IC_{50} of 1.42 μg/mL. Docking studies was also studied the result showed a potent inhibitory activity in tumor growth may be a potential anticancer agent. [1].

2.2 Atom based 3D-QSAR and Docking Studies of Chalcone Derivatives as Tubulin Inhibitors.

Naresh kandakatla et al (2014) designed a series of chalcone derivatives, pharmacophore, docking and Atom based QSAR studies were carried out for these derivatives. The QSAR results explain the electron withdrawing, positive, negative ionic and hydrophobic groups are crucial for the tubulin inhibition. Tubulin was an attractive target for anticancer drug and their inhibition were used in the various cancer treatments [2].

2.3 Chalcone synthase and its functions in plant resistance.

Dao T.T.H et al (2011) discussed the Chalcone Synthase and its function in plant resistance. Chalcone synthase it was a key enzyme for the flavonoid and isoflavonoid in bio-synthetic pathway. CHS gene expression is induced in plants under stress conditions such as UV light, bacterial or fungal infection. CHS expression causes accumulation of flavonoid and isoflavonoid phytoalexins and is involved in the salicylic acid defense pathway [3].

2.4 Synthesis of chalcone analogues with increased antileishmanial activity.

Paula Boeck et al (2006) synthesized eighteen analogues of active natural chalcones and the synthesized chalcones were tested for selective activity against promastigotes and intracellular amastigotes of Leishmania amazonensis in vitro. In these three of analogues which contains nitro, fluorine, bromine groups showed an increased selectivity against the parasites when compared with the natural chalcones. The nitrosylated chalcone was tested in infected mice and it was found to be effective as Pentostan reference drug [4].

2.5 Synthetic chalcones as efficient inhibitors of Mycobacterium tuberculosis protein tyrosine phosphatase PtpA

Louise Domeneghini Chiaradia et al (2008) prepared a 38 synthetic chalcones and the synthesized chalcones were assayed for their potential inhibitory action towards a protein tyrosine phosphatase from Mycobacterium tuberculosis – PtpA. Five compounds presented the good activity. The structure-activity analysis shows that the major factor for the activity was the model planarity or hydrophobicity and the nature of substituents [5].

2.6 The synthesis of 4,6-diaryl-2-pyridones and their bioactivation in CYP1 expressing breast cancer cells.

Ketan Ruparelia C et al (2019) developed anti-cancer prodrugs which were activated by the cytochrome P450 (CYP) 1B. A library of 4,6-diaryl-2-pyridones was synthesized in yields of 6–60% from the corresponding chalcones. The synthesized derivatives showed antiproliferative activities in human breast cancer cell lines which express CYP1B1 and CYP1A1, showing little toxicity towards a non-tumour breast cell line with no CYP expression [6].

2.7 Synthesis and biological evaluation of aromatic enones related to curcumin.

Thomas Philip Robinson et al (2005) reported a series of synthesis of structurally related compounds utilizing a substituted chalcone using Curcumin as a lead compound for anti-angiogenic analog design. The synthesized compound was tested via an established SVR cell proliferation assay. The resulting synthesized compound was equal to curcumin ability to inhibit endothelial cell growth in vitro. Because of their commercial availability and straight forward preparation these compounds were attractive leads for developing future angiogenic inhibitors [7].

2.8 The Design, Synthesis, in vitro Biological Evaluation and Molecular Modeling of Novel Benzenesulfonate Derivatives Bearing Chalcone Moieties as Potent Anti-microtubulin Polymerization Agents.

Yu-Ning et al.(2015) prepared 3,4- dimethoxybenzenesulfonate derivatives containing a chalcone structure and evaluated for their antiproliferative activities against HepG-2,MCF-7 and HeLa cell lines with IC_{50}– 123.9nM, 150.4nM and 131.4nM respectively, from this study they strongly commented upon the optimized stratagem for chalcone ligands targeting the colchicines binding site on microtubules, explaining the attribution that the analogues were designed upon the structure of chalcone and combretastatin A-4 [8].

2.9 Discovery of Biarylaminoquinazolines as Novel Tubulin Polymerization Inhibitors.

Giovann Marzaro et al. (2014) studied the discovery of Biarylaminoquinazolines as Novel Tubulin Polymerization Inhibitors, 4-biphenylaminoquinazoline multityrosine kinase inhibitors revealed an activity profile resembling that of known tubulin polymerization inhibitors. Novel 4-biarylaminoquinazoline analogues were synthesized and evaluated as inhibitors of several tyrosine kinases and of tubulin. Although compounds acted as dual inhibitors, the heterobiaryl analogues possessed only anti-tubulin properties and targeted the

colchicine site and the molecular modeling studies allowed the rationalization of the pharmacodynamic properties of the compounds [9].

2.10 Optimization of 4‑(N‑Cycloamino)phenylquinazolines as a Novel Class of Tubulin-Polymerization Inhibitors Targeting the Colchicine Site.

Xiao-Feng Wang et al (2014) introduced 4-(N-Cycloamino) phenylquinazolines as a Novel Class of Tubulin-Polymerization Inhibitors Targeting the Colchicine Site. The compounds were evaluated in cytotoxicity and tubulin inhibition assays, resulting in the discovery of new tubulin- polymerization inhibitors. 7-Methoxy- 4-(2-methylquinazolin- 4-yl)-3,4- dihydroquinoxalin- 2(1H)-one, the most potent compound, exhibited high in vitro cytotoxic activity (GI50 1.9−3.2 nM), significant potency against tubulin assembly (IC50 0.77 μM), and substantial inhibition of colchicine binding (99% at 5 μM) [10].

2.11 Synthesis, electrochemical and biological studies on novel coumarin-chalcone hybrid compounds.

Fernanda Perez-Cruz et al (2013) synthesized a series of novel hydroxyl coumarin chalcone hybrid compounds and characterized by using ESR, CV based on the result they have discussed the oxidation mechanism for the target compounds. The reported compound possesses high ORAC value (14.1) and also has good scavenging capacity with cytoprotective activity [11].

2.12 Cellular and molecular mechanisms activating the cell death processes by chalcones: Critical structural effects.

Pierre Champelovier et al (2013) studied the Cellular and molecular mechanisms activating the cell death processes by chalcones: Critical structural effects of Chalcones are naturally occurring compounds with diverse pharmacological activities. Chalcones derive from the common structure: 1,3- diphenylpropenone and providing evidences that minor structural difference could lead to important difference in mechanistic effect [12].

2.13 Design, synthesis and biological evaluation of millepachine derivatives as a new class of tubulin polymerization inhibitors.

Guangcheng Wang et al (2013) introduced Millepachine derivatives as a new class of tubulin polymerization inhibitors. A series of novel tubulin polymerization inhibitors have been synthesized and evaluated for their in vitro and in vivo biological activities. Among these compounds, Millepachine displayed strong antiproliferative activity against several tumor cell lines (IC_{50} = 0.15–0.62 lM). The proposed compound was also shown to arrest cells in the G2/M phase of the cell cycle and inhibit the polymerization of tubulin. Molecular docking studies suggested that the compound binds into the colchicine binding site of tubulin and it's a promising new antimitotic compound for the treatment of cancer [13].

2.14 Synthesis, Biological Evaluation, and Molecular Modeling of Chalcone Derivatives as Potent Inhibitors of Mycobacterium tuberculosis Protein Tyrosine Phosphatases (PtpA and PtpB).

Louise Domeneghini Chiaradia et al (2012) synthesized a new series of napthylchalcones and they identified as inhibitors of Mycobacterium tuberculosis (Mtb) protein tyrosine phosphates with the help of molecular modeling investigations. From the study of Structure activity relationship, they proposed the compound as a potential anti TB drugs [14].

CHAPTER -3

AIM AND SCOPE

3.1 Aim

- To synthesis (*E*)-3-(benzo[*d*][1,3]dioxol-5-yl)-1-(3,4-dimethoxyphenyl)prop-2-en-1-one from 3, 4 Dimethoxy acetophenone and Piperonal under basic condition.
- To characterize the compounds using various spectroscopic methods such as UV-Visible, FT-IR, FT-Raman, ^{1}H, ^{13}C $\{^{1}H\}$ & DEPT 135 NMR and HRMS.
- To study the molecular structure of the compound using single crystal X-ray diffraction studies.
- To study the molecular docking to study the interaction between receptor of SARS-CoV-2 main protease and the synthesized compound.

3.2 Scope

- The detailed spectral assignments for the synthesized compounds were made
- Crystallographic structure of compound 2 was solved and it was not planar. The structure has been deposited in CCDC database.
- From the molecular docking studies, it's evident that the compound may considered as a potential candidate for *in vitro* anti-viral studies.

CHAPTER - 4

MATERIALS AND METHODS

4.1 Materials

Solvents were dried according to the standard procedure [1]. 3, 4 Dimethoxy acetophenone was purchased from Spectrochem Pvt. Ltd., Mumbai. Pipernol was purchased from Sigma-Aldrich. NaOH purchased from SRL. All the chemicals were used without further purification.

4.2 Methods

4.2.1 SciFinder

SciFinder is developed by Chemical Abstracts Service (CAS), it is widely used database for the chemical literature it is searchable by substance by name or CAS registry number, topic, author, reactions, or editor can be used to draw the structure. It is an major research tool for various field which includes Chemistry, Bio-Chemistry, Chemical engineering, Material science, Nanotechnology, Physics, environmental science and other science and engineering disciplines.

4.2.2 CSD ConQuest

Conquest is US based software which was developed to benefit the oracle database customers. Conquest provides database programming, visualization, documentation, advanced support of legacy PS/SQL code analysis and database security.

4.3 Physical Measurements

UV-Visible Spectra was recorded using Shimadzu UV-1800 Spectrophotometer. FT-IR spectrum was recorded on a Perkinelmer SPECTRUM ONE FT-IR spectrophotometer as KBr pellet in the frequency range of 400-4500 cm^{-1}. The FT-Raman spectra were recorded in the BRUKER RFS 27 MultiRAM Standalone FT-Raman Spectrometer in the frequency range 50–4000 cm^{-1}. The Laser source is Nd YAG laser source operating at 1064 nm line with 100 mW powers. The frequencies of all sharp bands are accurate to ±1 cm^{-1}. HRMS data were obtained from Bruker Impact HD ESI Q-TOF high resolution mass spectrometer. The ^{1}H and ^{13}C $\{^{1}H\}$ NMR spectra were recorded in $CDCl_3$ solution

on a Bruker BRUKER AVIII 500 MHz spectrometer (Bruker BioSpin AG, Fallanden, Switzerland) using TMS as internal standard.

4.4 Single Crystal XRD

Single crystal of compound **1** suitable for X-ray diffraction studies were grown at room temperature from ethanol solution by slow evaporation. Diffraction data were collected on a Bruker Kappa APEX-II CCD CCD diffractometer using graphite monochromated MoKα radiation (λ = 0.71073 Å). After data integration with program SAINT, absorption corrections with the multi-scan method and program SADABS were applied [2]. The structures were solved by direct methods (SHELXS-97) and refined by full – matrix least squares fitting based on F^2 using the program SHELXL-97 [3]. All non-hydrogen atoms were refined with anisotropic displacement parameters. All H atoms were located by difference Fourier syntheses and were then included in the refinement mostly with idealized geometry riding on the atoms to which they were bonded.

4.5 Synthesis of Chalcone

A mixture of piperonal (0.083g, 0.0555 mole) and 3,4 dimethoxy acetophenone (0.1 g, 0.0555 mole) was dissolved in 10 mL of ethanol in 50 mL round bottomed flask. Then 10% NaOH (330 μL) was added drop wise to the reaction mixture. The reaction was monitored by TLC and stirred at 25^{o}C for about 4 hours. After the reaction completion, the solvent was reduced to 5 mL using the distillation method. Then Dichloromethane (3 mL) and distilled water (5 mL was added to the reaction residue. The mixture was kept for about of two days for crystallization. Once the crystal is formed it was filtered using filter paper washed several times with water and ethanol dried and weighed. The yield of the product was about 50%.

4.5.1. (E)-3-(benzo[d][1,3]dioxol-5-yl)-1-(3,4-dimethoxyphenyl)prop-2-en-1-one.

m.p.: °C; Yield: 70 mg, 50%. ^{1}H NMR (500 MHz, $CDCl_3$) δ 3.97 (s, 3H), 3.98 (s, 3H), 6.03 (s, 2H), 6.85 (d, *J* = 8.0 Hz, 1H), 6.93 (d, *J* = 8.4 Hz, 1H), 7.13 (dd, *J* = 8.2, 1.7 Hz, 1H), 7.18 (d, *J* = 1.7 Hz, 1H), 7.40 (d, *J* = 15.5 Hz, 1H), 7.62 (d, *J* = 2.0 Hz, 1H), 7.67 (dd, *J* = 8.4, 2.0 Hz, 1H), 7.74 (d, *J* = 15.4 Hz, 1H). ^{13}C NMR (101 MHz, $CDCl_3$) δ 56.18, 56.22, 101.73, 106.75, 108.79, 110.09, 110.90,

119.82, 122.98, 125.19, 129.67, 131.61, 143.97, 148.50, 149.35, 149.87, 153.29, 188.61. HR-ESI-MS (Calculated for $C_{18}H_{16}O_5$ = 312.3166) ($[M+H]^+$ = 313.1071 Da) : 313.1073 error : - 0.5 ppm.

4.6 Molecular Docking

The three dimensional (3D) structure of the SARS-CoV-2 Main protease (**PDB ID: 6LU7**) were obtained from the protein data bank. Synthesized chalcone compound structures were available in the PubChem database. The tautomers for each of these compounds were generated and optimized (ligprep, v2.3). The optimized compounds were subjected to docking with the native structures of SARS-CoV-2 using widely used docking program Autodock [4]. The docking was performed for all the small molecules by keeping the ligand as flexible. The grid was placed at the interface region of the native structures of SARS-CoV-2 Main protease**.**

Before performing docking, polar hydrogen was added by using the Hydrogen module in AutoDock Tools (ADT) for native structures of Main protease of SARS-CoV-2 followed by assigning Kollman united atom partial charges. The docking of native structures of SARS-CoV-2 with the chalcone was carried out using the empirical free energy function and the Lamarckian genetic algorithm, applying a standard protocol with an initial population of 150 randomly placed individuals. A maximum number of 2.5 x 10^7 energy evaluations, a mutation rate of 0.02, and a crossover rate of 0.08, where the average of the worst energy was calculated over a window of the previous 10 generations, were involved to standardize the protocol. Genetic Algorithm of 20 independent docking cycles was carried out for each ligand. The grid maps representing the proteins in the actual docking process were calculated with Auto Grid. The grids were chosen to be sufficiently large to include the active site. The dimensions of the grids x-, y-, z-axes were set to 20 Å x 20 Å x 20 Å for the receptors. The grid spacing was set at 0.425 Å for Main protease of SARS-CoV-2. The entire small molecule bound to Main protease of SARS-CoV-2 was examined for binding energy and also for specific and non-specific interacting residues. The docked conformations were visualized using BIOVIA Discovery Studio Visualizer. The conformation with lowest binding free energy was used for further analysis.

CHAPTER 5

RESULTS AND DISCUSSIONS

5.1 Synthesis

The synthesis of chalcone **1** was summarized in scheme 1 shown below. The compound 1 was synthesized by reacting 3, 4 Dimethoxy acetophenone with piperonal in ethanol as a solvent through Claisen-Schmidt condensation reaction under the basic condition in good yield. The synthesized compounds were found to be soluble in $CHCl_3$, CH_2Cl_2, CH_3CN, DMSO, DMF and C_2H_5OH. The FT-IR, FT-Raman, 1D NMR and HR-ESI-MS data of these compounds are in good agreement with the proposed chemical structure and molecular formula.

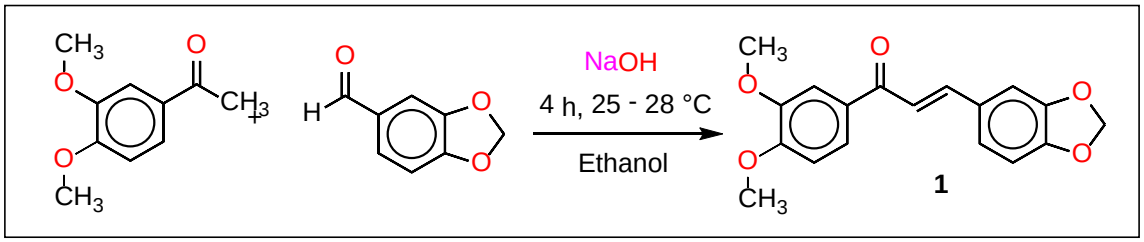

Scheme 1 Synthesis of compound 1

5.2 UV-Visible spectroscopy

The UV-Visible spectrum of the synthesized compound **1** was measured in the range of about 200 – 800 nm using chloroform as a solvent. The compound **1** contains α,β-unsaturated carbonyl group, it is expected to show two absorption bands pertaining to the n-π* and π-π* transitions. The compound **1** showed strong absorption band at 359 nm which was due to the n-π* transition and the weak band around 213- 278 nm which was due to the π-π* transitions.

5.3 FT-IR Spectroscopy

The FT-IR spectrum (Fig. 2.1) of the synthesized product **1** showed a strong C=O stretching vibration at 1655 cm^{-1}. The lowering of carbonyl stretching vibration when it is compared to the starting material is due to the formation of α, β unsaturated double bond in s-*trans* form. The peak at 2954 cm^{-1} corresponds to the strong sp^3 C-H stretching of the methoxy (OCH_3) group. Similarly, the peak at 3074 cm^{-1} was due to the aromatic sp^2 C-H stretching of the alkene (C=C-H) group. The strong bands at 1580 - 1495 cm^{-1} were assigned to the aromatic C=C

stretching of the compounds. The peaks at the 789 and 766 cm^{-1} corresponds to C=C-H out plane bending. The presence of peak at 1458 - 1409 cm^{-1} corresponds to the inplane C-H bending of Methylene group. The peak at 1352 cm^{-1} corresponds to the C-H bending of Methyl group [1].

5.4 FT-Raman Spectroscopy

The FT-IR spectrum (Fig. 2.2) of the synthesized product **1** exhibit a very week C=O stretching vibration at 1657 cm^{-1}. The lowering of carbonyl stretching vibration when it is compared to the starting material is due to the formation of α, β unsaturated double bond in s-*cis* form. The peak at 2957 cm^{-1} corresponds to the strong sp^3 C-H stretching of the methoxy (OCH_3) group. Similarly the peak at 3067 cm^{-1} was due to the aromatic sp^2 C-H stretching of the alkene (C=C-H) group. . The strong bands at 1593-1580 cm^{-1} were assigned to the aromatic C=C stretching of the compounds. The peaks at the 771 and 717 cm^{-1} corresponds to C=C-H out plane bending. The presence of peak at 1445.06-1414.28 cm^{-1} corresponds to the inplane C-H bending of Methylene group. The peak at 1359-1320 cm^{-1} corresponds to the C-H bending of Methyl group [2].

5.5 NMR spectroscopy

The ^1H, ^{13}C $\{^1H\}$ and DEPT135 NMR spectrum were recorded for the compound **1** with $CDCl_3$ as the solvent. In ^1H NMR spectrum, two singlets observed at 3.97, and 3.98 ppm, with integral value of three was assigned to Methoxy methyl (OC**H₃**) protons. A singlet at 6,03 ppm with two proton count is due to methylene group. The olefinic protons appeared as expected as two doublets at 7.40 and 7.74 ppm with *J* value of 15 Hz ca. This confirms that the olefinic protons are *trans* to each other. The aromatic protons of both rings appeared in the range of 6.84 – 7.62 ppm with AMX type splitting pattern. In carbon NMR spectrum (Fig. 3.3), the carbonyl carbons resonance was observed at 186.61 ppm. The olefinic carbons C8 and C9 unsaturated carbonyl compound appeared at 125 and 148 ppm respectively. Signals due to two methoxy carbons OCH_3 observed at 56 ppm. The resonance of methylene carbons (CH_2) were identified using DEPT135 NMR spectrum at 101 ppm as negative peak. The individual assignments of protons and carbon resonances were tabulated in Table 2.1 and 2.2 respectively

5.6 Mass spectroscopy

The acetonitrile solution of **1** was used to record the High resolution ESI MS spectrum in positive mode. The mass peak observed as $[M+H]^+$ at m/z 313.1075 for the compound **1** (Fig. 5.1). A good agreement was obtained for calculated m/z values and experimental m/z values for $[M+H]^+$ ions which indicates the purity of the synthesized compound.

5.7 X-ray crystallography

The compound **1** crystallize in Monoclinic crystal system (Space group: $P2_1/c$) with four molecules (Z = 4) in the unit cell. The ORTEP diagram is presented in Fig. 6.1. Data collection, structure solution and refinement details are given in Table 3.1. The structure was determined with R value of 3.9 %. Crystallographic data file has been deposited in Cambridge Structural Database. The bond lengths and bond angles of the compounds is given in Table 3.2. Table 3.3 shows the torsion angles for compound **1**. The electronegative Oxygen atom forms hydrogen bonds with C-H a group which in turn leads to the formation network in the crystalline solid structure (Fig. 6.2). The details of Hydrogen bonds of compound 1 was shown in Table 3.4

5.8 Molecular Docking

The docking simulation of chalcone **1**, tightly bound with the active site of the SARS-CoV-2 Main protease. Upon the examination of docking features in which the chalcone has the lowest binding energy (-6.1 kcal/mol) and established the five hydrogen bonding and the residue is THR25, CYS145, GLY143, SER144 and GLU166 respectively. The three hydrogen bond between the of carbonyl oxygen atom with hydrophobic residue of GLY143 (bond distance 2.11 Å) and polar residue of SER144 and CYS145 (bond distance 2.39 Å and 2.40 Å). Fourth hydrogen bond is oxygen atom (O3) of methylene di oxy ring with polar residue THR25 (bond distance 2.53 Å) and the fifth hydrogen bond was formed in between the oxygen (O4) in methoxy group charged residue of GLU166 (bond Distance 2.06 Å). Furthermore, the following residues were mainly involved in hydrophobic and polar residue Vander Waals interactions LEU141, MET49, ASN142, THR45, THR24 and THR26 (Fig. 6.1).

CONCLUSION

In the present study, chalcone **1** was synthesized by reacting 3, 4 dimethoxy acetophenone with pipernol under basic condition and characterized by spectroscopic and single crystal X-ray diffraction techniques. Vibration property of the molecule was studied by FT-IR and FT-Raman spectroscopy. The crystal structure of chalcone **1** was determined by the single crystal XRD method. The compound **1** crystallized in the monoclinic system with space group $P2_1/c$. Crystal structure based molecular docking studies was performed *in silico* to study the binding mode of the chalcone **1** with Main Protease of SARS CoV-2 (6LU7) downloaded from the PDB website. The binding of ligand with receptor was stabilized by hydrogen bonding, van der Waals interactions, Carbon Hydrogen bond, alkyl, and pi-alkyl interactions. Docking studies showed that compounds bind effectively to the Main Protease of SARS-CoV-2 (6LU7). Hence, this chalcone can be taken further tested for *in vitro* anti-viral studies.

REFERENCE

CHAPTER - 1

[1] Chavan B.B, Gadekar A.S, Mehta P.P, Vawhal P.K, Kolsure A.K, Chabukswar A.R, Synthesis and Medicinal Significance of Chalcones- A Review, Asian Journal of Biomedical and Pharmaceutical Sciences, 6(56), 2016, 01-07.

[2] Sunil T, Samson M, Ofentse P, Shivaji T, Pravin K and Rajandra P, Biological Role of Chalcones in Medicinal Chemistry intechopen. 2020 91626.

[3] Amarajothi D, Mercedes A and Hermenegildo G, Claisen–Schmidt Condensation Catalyzed by Metal-Organic Frameworks, Advanced Synthesis Catalysis 2010, 352, 711 – 717 2010.

[4] Kritika K, Rajiv G Bioavailability enhancers of herbal origin: An overview, Asian Pacific Journal of Tropical Biomedicine, 3(4), 2013, 253-266.

[5] Balaji M, Brahmanaidu P, Venkata Rao C, Ramavat Ravindar N, Harishankar N, Pothani S, Saravanan G and Sathibabu Uddandrao V.V, Antiobesity potential of Piperonal:promising modulation of body composition, lipid profiles and obesogenic marker expression in HFD-induced obese rats, Nutrition & Metabolism (2017) 14:72.

[6] Huan Q, Min L, Hui X, Piperine: Bioactivities and Structural Modifications, Mini-Reviews in Medicinal Chemistry, 15(2), 2015, 145-56.

[7] Sagar K, A Review on Anticonvulsant activity of 1, 3-Benzodioxole ring system based compounds, International Journal of Pharmaceutical Sciences and Research, Vol. 4(9), 2013, 3296-3303.

CHAPTER-2

[1] Hui Z, Jia-Jia L, Jian S, Xian-Hui Y, Ting-Ting Z, Xiang L, Hai-Bin G, Hai-Liang Z, Design, synthesis and biological evaluation of novel chalcone derivatives as antitubulin agents, Bioorganic & Medicinal Chemistry 20,2012 3212–3218.

[2] Naresh K, Geetha R, Karthikeyan J, Rajasekhar C, Pharmacophore Modeling, and Atom based 3D-QSAR and Docking Studies of Chalcone Derivatives as Tubulin Inhibitors, Orient Journal of Chemistry, 30(3), 2014, 1083-1098.

[3] Dao T.T.H, Linthorst H.J.M, Verpoorte R, Chalcone synthase and its functions in plant resistance, Phytochemistry Reviews 10, 2011, 397-412.

[4] Paula B, Camila A.B.F, Paulo C.L, Rosendo A.Y, Valdir C.F, Eduardo C.T.S and Bartira R.B, Synthesis of chalcone analogues with increased antileishmanial activity, Bioorganic & Medicinal Chemistry, 14, 2006, 1538–1545.

[5] Louise D.C, Alessandra M, Marcela P, Javier V, Marlon N.S.C, María E.Z, Andrea V, Ricardo J.N, Rosendo A.Y, Hernan T, Synthetic chalcones as efficient inhibitors of Mycobacterium tuberculosis protein tyrosine phosphatase PtpA, Bioorganic & Medicinal Chemistry Letters, 18, 2008, 6227–6230.

[6] Ketan C.R, Sabahat L, Dyan N.A, Nicola E.W, Randolph R.J.A, Gerard A.P, Kenneth J.M.B, The synthesis of 4,6-diaryl-2-pyridones and their bioactivation in CYP1 expressing breast cancer cells, Bioorganic & Medicinal Chemistry Letters, 29 2019, 1403–1406.

[7] Thomas P.R, Richard B.H, Tedman J.E, Jack L.A, David J.G and Phillip Bowen J, Synthesis and biological evaluation of aromatic enones related to curcumin, Bioorganic & Medicinal Chemistry 13, 2005, 4007–4013.

[8] Yu-Ning S, Lin L, Han-Yue Q, Wen-Yan Z, Yong Q, Hai-Liang Z, The Design, Synthesis, in vitro Biological Evaluation and Molecular Modeling of Novel Benzenesulfonate Derivatives Bearing Chalcone Moieties as Potent Anti-microtubulin Polymerization Agents, RSC Advances, 5, 2015, 23767-23777.

[9] Giovanni M, Antonio C, Alessandro F, Paola B, Ignazio C, Maria T.C, Giuseppe L.R, Ruoli B, Romano S, Ernest H and Adriana C, Discovery of Biarylaminoquinazolines as Novel Tubulin Polymerization Inhibitors, Journal of Medicinal Chemistry, 57, 2014, 4598−4605.

[10] Xiao-Feng W, Fang G, Emika O, Wanjun Guo, Lili W, Dong-Qing Z, Sheng-Biao W, Li-Ting W, Ernest H, Dexuan Y, Linna L, Keduo Q, Susan L. Morris N, Shoujun Y, Kuo- Hsiung L, and Lan X, Optimization of 4-(N-Cycloamino)phenylquinazolines as a Novel Class of Tubulin-Polymerization Inhibitors Targeting the Colchicine Site, Journal of Medicinal Chemistry, 5, 2014, 1390−1402.

[11] Fernanda P.C, Saleta V.R, Maria J.M, Alejandra H.M, Frederick A.V, Amlan D, Bhavani G Claudio O.A, Lourdes S and Eugenio U, Synthesis, electrochemical and biological studies on novel coumarin-chalcone hybrid compounds Journal of Medicinal Chemistry, 56 (15), 2013, 6136–6145.

[12] Pierre C, Xavier C, Florence H.P, Sabrina V, Catherine G, Francois L, Jean B, Ahcene B, Cellular and molecular mechanisms activating the cell death processes by chalcones: Critical structural effects, Toxicology *in vitro*, 27, 2013, 2305–2315.

[13] Guangcheng W, Fei P, Dong C, Zhuang Y, Xiaolei H, Juan L, Wenshuang W, Lin H, Liang M, Jinying C, Yun S, Mingli X, Aihua P, Yuquan W, Lijuan C, Design, synthesis and biological evaluation of millepachine derivatives as a new class of tubulin polymerization inhibitors, Bioorganic & Medicinal Chemistry, 21, 2013, 6844–6854.

[14] Louise D.C, Priscila G.A.M, Marlon Norberto N.S.C, Rafael V.C.G, Gabriela E, Adriano D.A, Rosendo A.Y, Javier V, Ricardo J.N and Hernan T, Synthesis, Biological Evaluation, And Molecular Modeling of Chalcone Derivatives As Potent Inhibitors of Mycobacterium tuberculosis Protein Tyrosine Phosphatases (PtpA and PtpB), Journal of Medicinal Chemistry, 55, 2012, 390−402.

CHAPTER - 4

[1] Vogel, Arthur I. (Arthur Israel). Vogel's Textbook of Quantitative Chemical Analysis. Harlow, Essex, England: New York: Longman Scientific & Technical; Wiley, 1989.

[2] Bruker (2003), Bruker AXS Programs: SMART, Version 5.629; SAINT, Version 6.45; SADABS, Version 2.10; XPREP, Version 6.14, Bruker AXS Inc., Madison, WI, USA.

[3] Sheldrick. G (2008) A short history of SHELX. Acta Cryst, 64 A, 112-122.

[4] Morris, G. M., Huey, R., Lindstrom, W., Sanner, M. F., Belew, R. K., Goodsell, D. S. and Olson, A. J. (2009) Autodock4 and AutoDockTools4: automated docking with selective receptor flexiblity. Journal of Computational Chemistry, 16, 2009, 2785-2791.

CHAPTER 5

[1] Larkin P,Infrared and Raman Spectroscopy, 2011, 230.

[2] Daimay Lin-Vien Norman Colthup William Fateley Jeanette Grasselli,The Handbook of Infrared and Raman Characteristic Frequencies of Organic Molecules,1st Edition,1991,503.

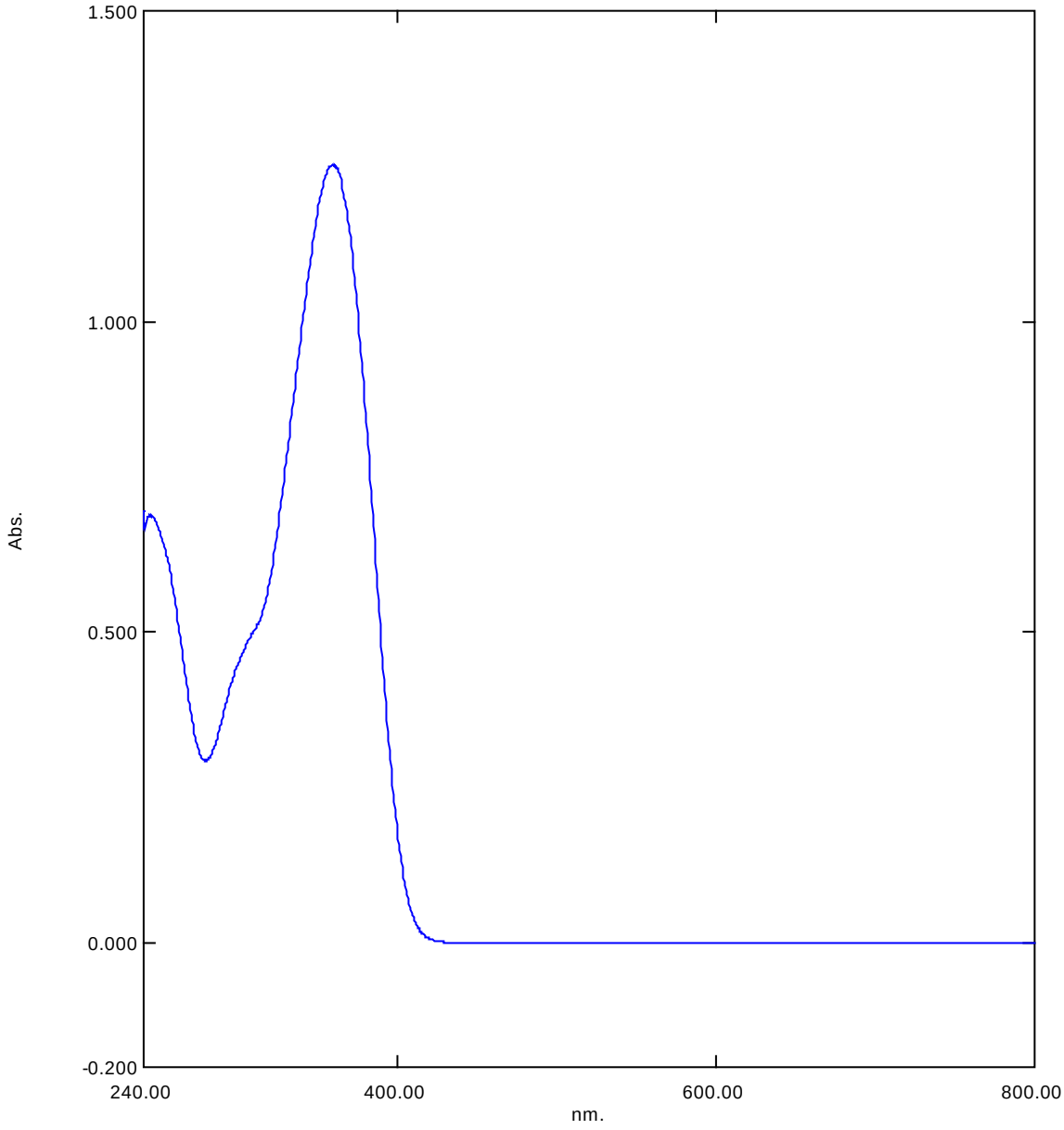

Figure 1.1 UV-Visible spectra of compound 1 in Chloroform

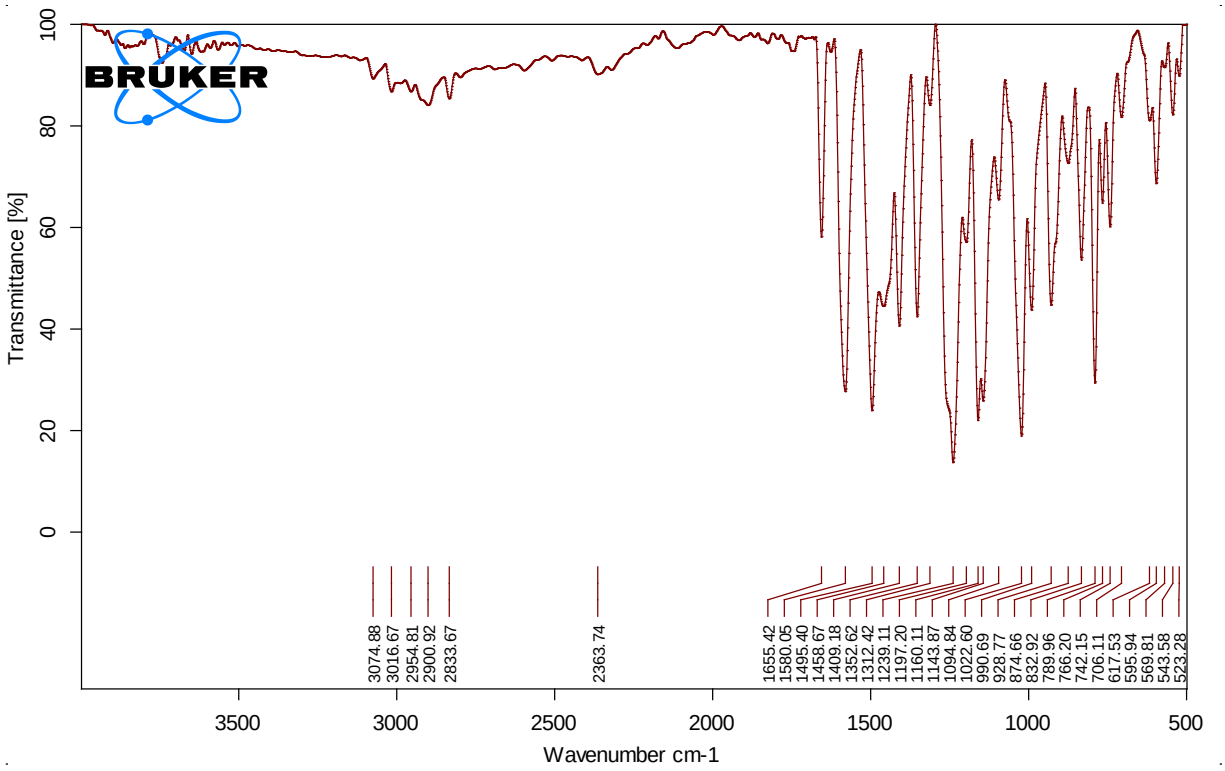

Figure 2.1 FT-IR spectrum of compound 1

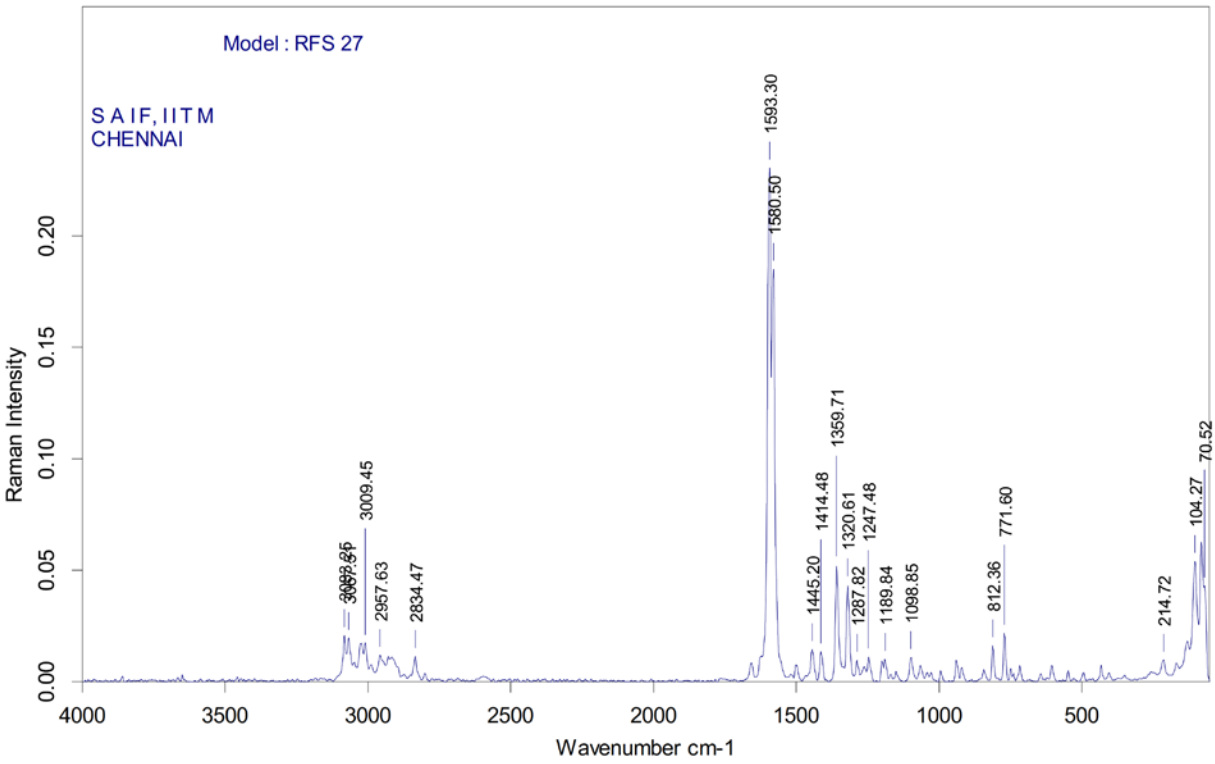

Figure 3.1 FT-Raman spectrum of compound 1

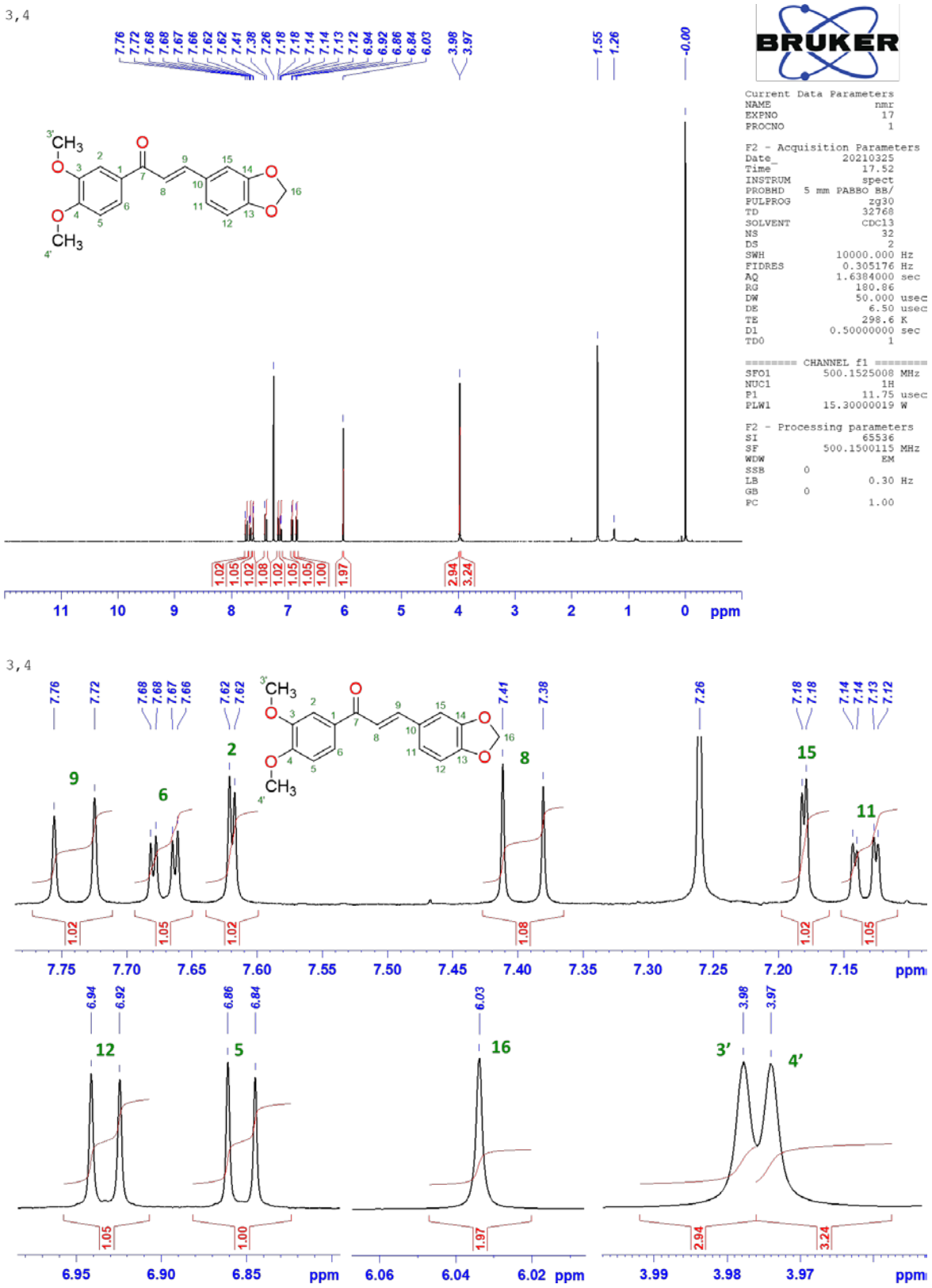

Figure 4.1 ^{1}H NMR spectrum of compound 1

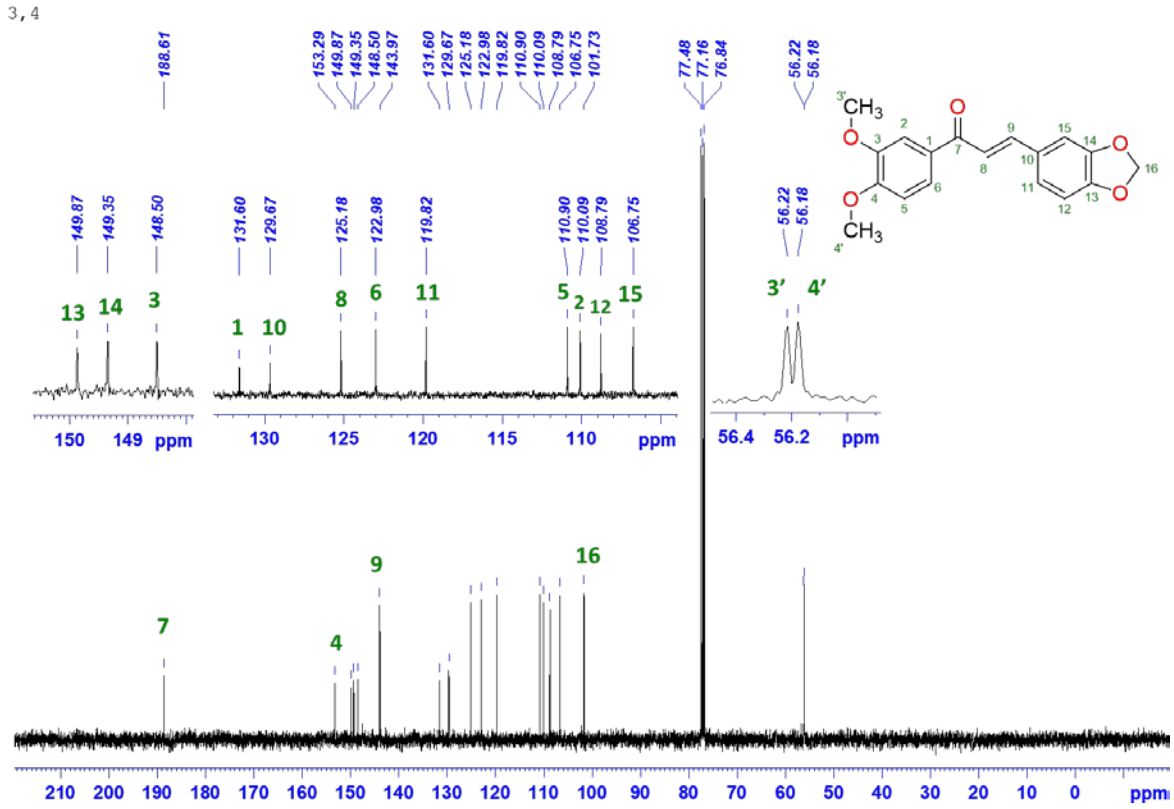

Figure 4.2 ^{13}C NMR spectrum of compound 1

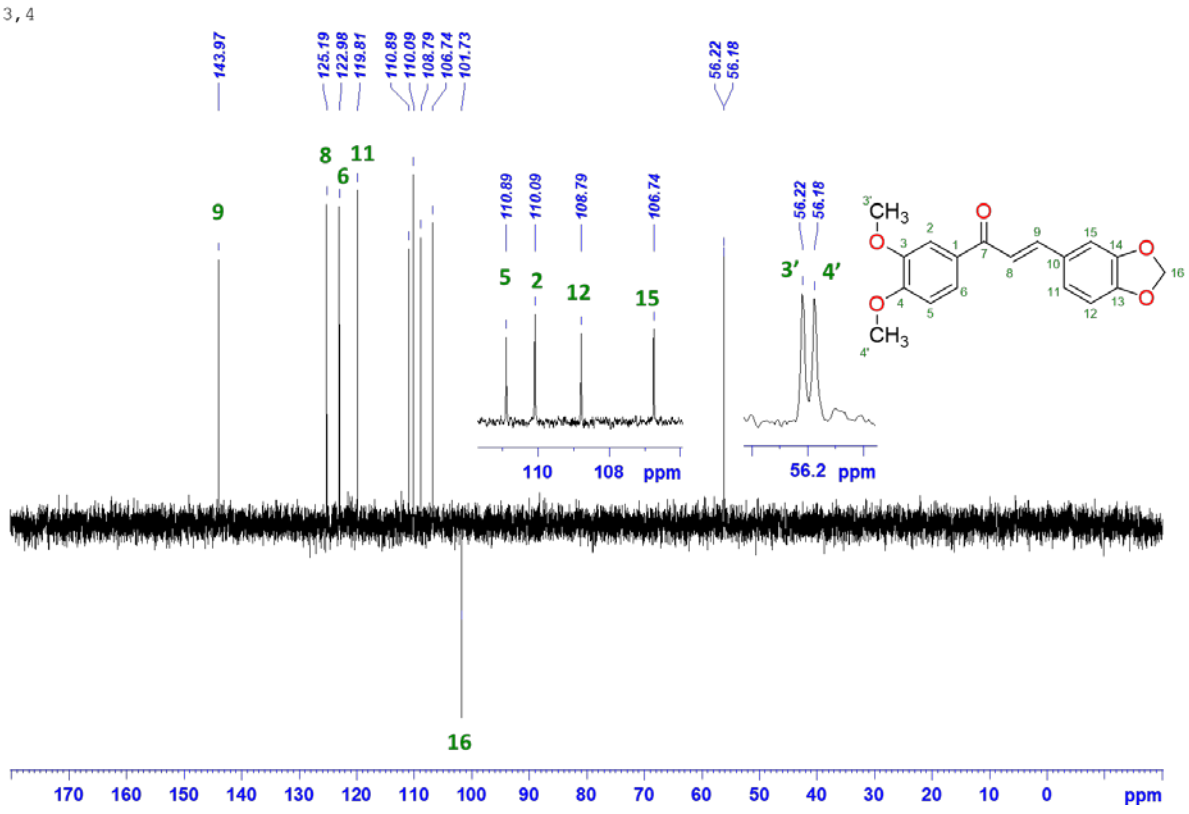

Figure 4.3 DEPT135 NMR spectrum of compound 1

Mass Spectrum SmartFormula Report

Analysis Info

Analysis Name	D:\Data\HRMS\34.d	Acquisition Date	4/9/2021 2:53:50 PM
Method	Harish HRMS.m	Operator	Demo User
Sample Name	34	Instrument	impact HD 1819696.00315
Comment			

Acquisition Parameter

Source Type	ESI	Ion Polarity	Positive	Set Nebulizer	2.0 Bar
Focus	Not active	Set Capillary	4500 V	Set Dry Heater	220 °C
Scan Begin	50 m/z	Set End Plate Offset	-500 V	Set Dry Gas	8.0 l/min
Scan End	1300 m/z	Set Charging Voltage	2000 V	Set Divert Valve	Waste
		Set Corona	0 nA	Set APCI Heater	0 °C

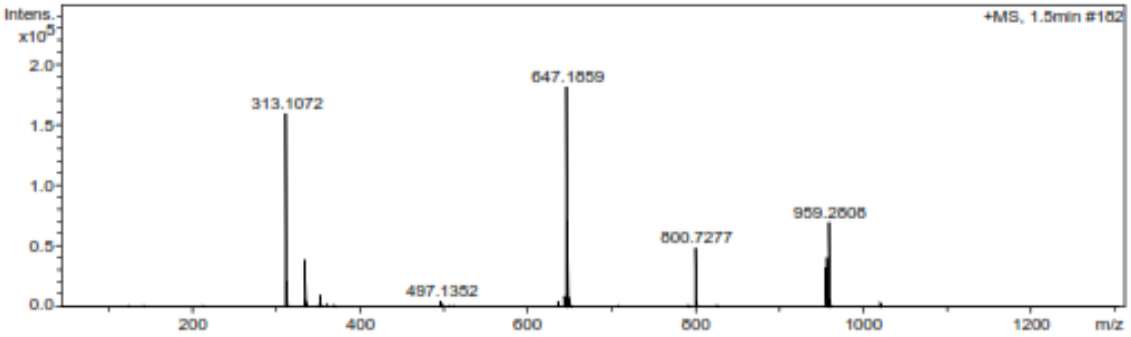

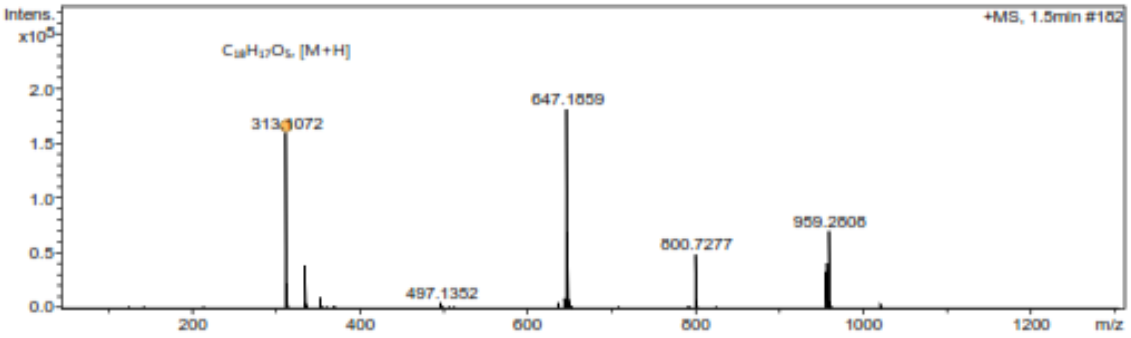

Meas. m/z	#	Ion Formula	m/z	err [ppm]	mSigma	# mSigma	Score	rdb	e⁻ Conf	N-Rule
313.1072	1	C18H17O5	313.1071	-0.5	36.6	1	100.00	11.0	even	ok

34.d

Bruker Compass DataAnalysis 4.4 printed: 4/9/2021 2:59:14 PM by: demo Page 1 of 1

Fig 5.1 ESI-MS spectrum of compound 1

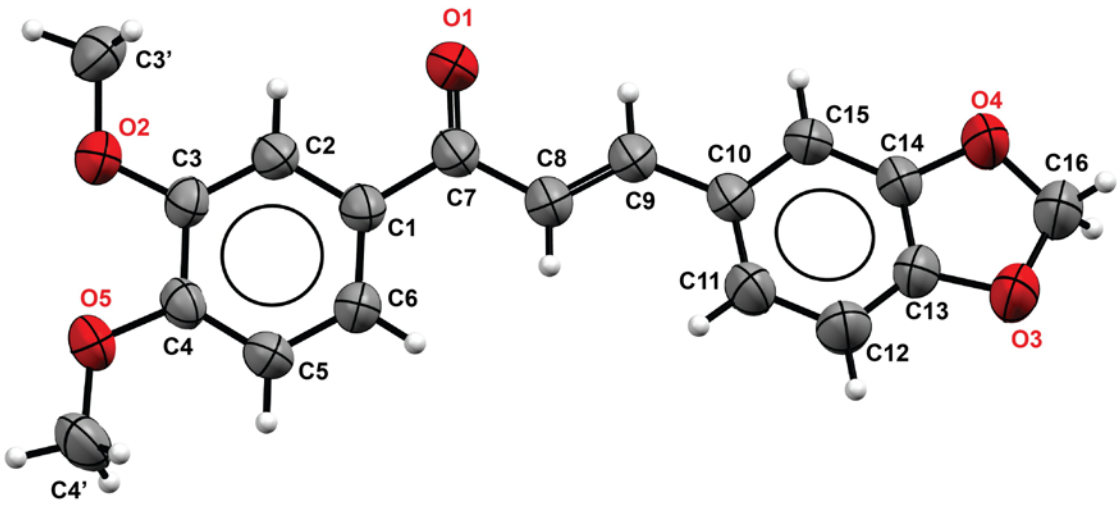

Figure 6.1 Thermal ellipsoidal plot of compound 1 showing the atomic labeling scheme and thermal ellipsoids at the 50% probability level

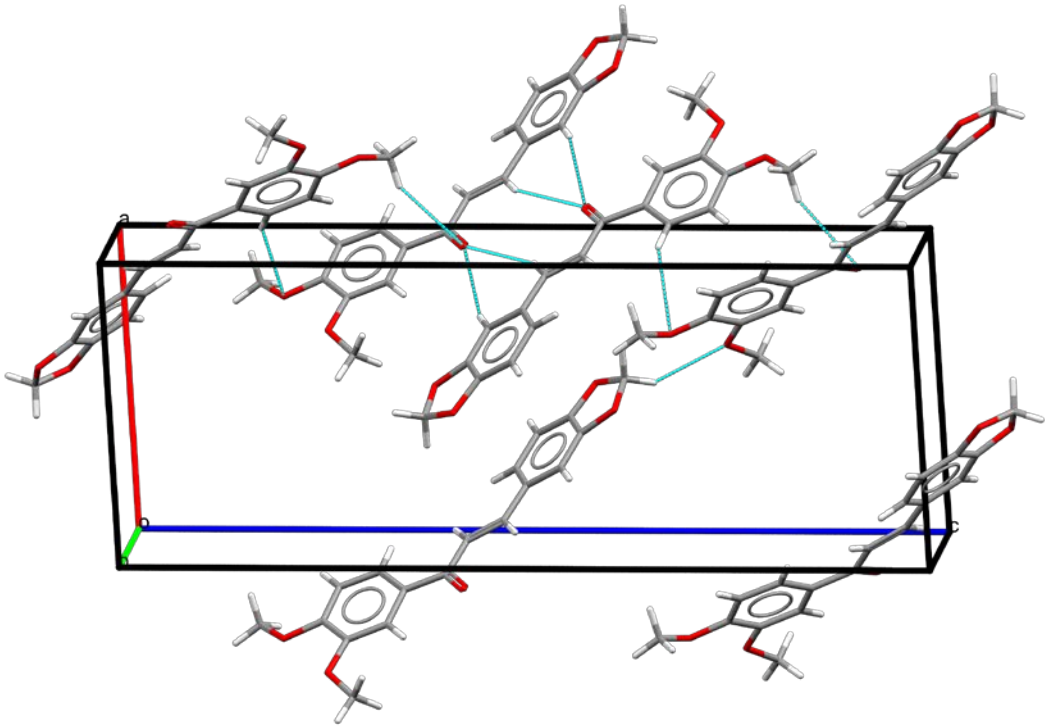

Figure 6.2 Crystal packing diagram of 1 in a unit cell

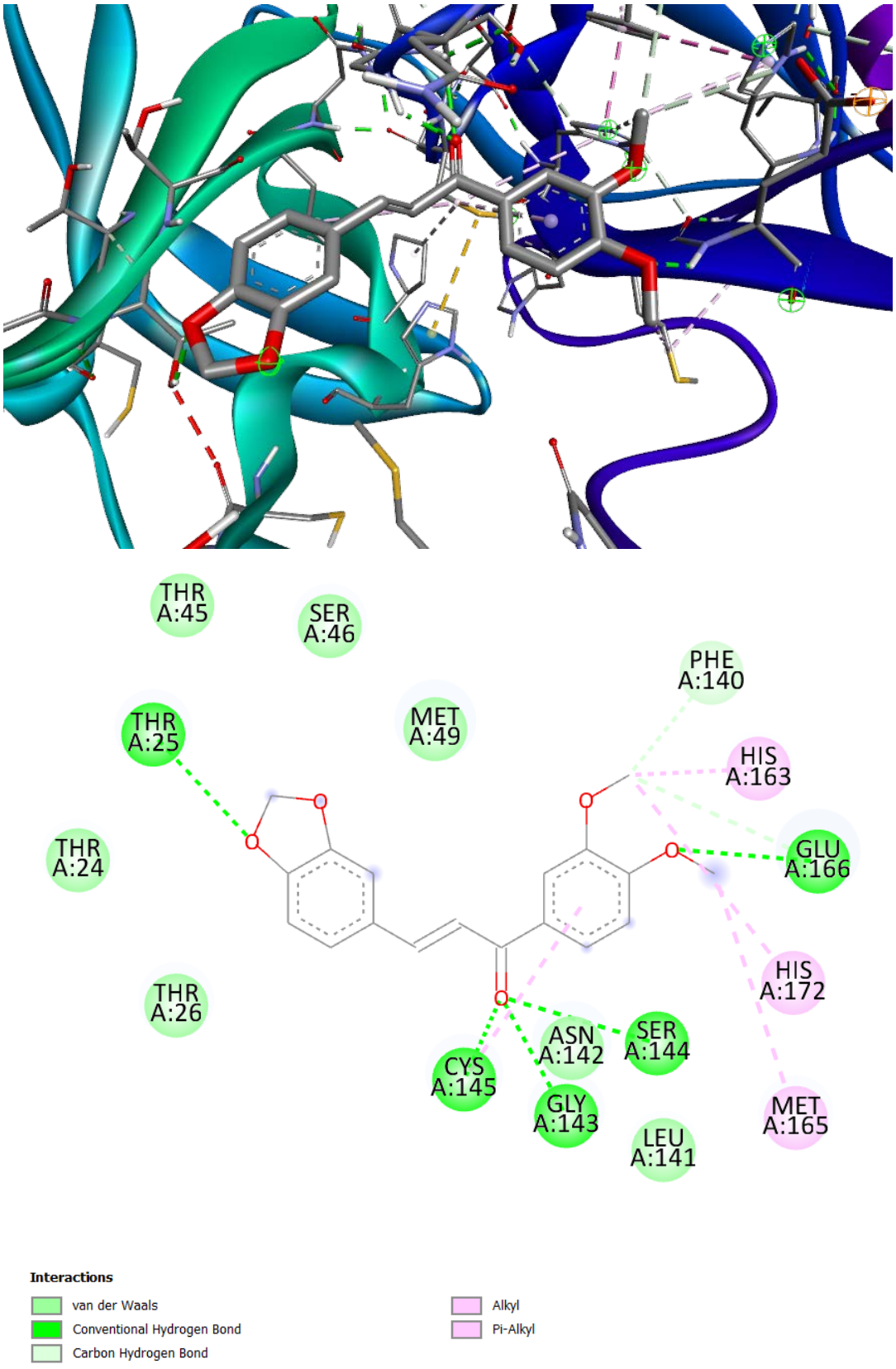

Figure 7.1 The binding mode between chalcone 1 and the binding site of the SARS-CoV-2 (PDB ID: 6LU7)

Table 1.1 FT-IR spectral assignment of compound 1

IR Frequency (cm^{-1})	ASSIGNMENT
3074 (m)	Aliphatic sp^3 C–H stretching
2954 (m)	Aromatic sp^2 C–H stretching
1655 (vs)	C=O stretching (α, β conjugated)
1580, 1495 (vs)	Aromatic C=C stretching
1458 (vs)	In plane C-H Methylene bending
1352 (vs)	C-H Methyl In plane bending
766, 789 (s)	Out of plane C=C-H bending

Table 1.2 FT-Raman spectral assignment of compound 1

RAMAN Frequency (cm^{-1})	ASSIGNMENT
3067 (m)	Aliphatic sp^3 C–H stretching
2957 (m)	Aromatic sp^3 C–H stretching
1655 (vw)	C=O stretching (α, β conjugated)
1593,1580 (vs)	Aromatic C=C stretching
1445 (m)	In plane C-H Methylene bending
1359 (m)	In plane C-H Methyl bending
771, 717 (w)	Out of plane C=C-H bending

Table 2.1 ^{1}H NMR spectral assignment of compound 1.

H's No.	δ_H (ppm)
H2	7.62 (d, *J* = 2.0 Hz, 1H)
H3'	3.98 (s, 3H)
H4'	3.97 (s, 3H)
H5	6.85 (d, *J* = 8.0 Hz, 1H)
H6	7.67 (dd, *J* = 8.4, 2.0 Hz, 1H)
H8	7.40 (d, *J* = 15.5 Hz, 1H)
H9	7.74 (d, *J* = 15.4 Hz, 1H).
H11	7.13 (dd, *J* = 8.2, 1.7 Hz, 1H)
H12	6.93 (d, *J* = 8.4 Hz, 1H)
H15	7.18 (d, *J* = 1.7 Hz, 1H)
H16	6.03 (s, 2H)

Table 2.2 ^{13}C NMR and DEPT 135 NMR spectral assignment of compound 1

Carbon No	δ_c(ppm)	DEPT 135
C1	131.60	**0**
C2	110.09	**– ve**
C3	148.50	**0**
C3'	56.22	**+ ve**
C4	153.29	**0**
C4'	56.18	**+ ve**
C5	110.90	**– ve**
C6	122.98	**0**
C7=O	186.61	**0**
C8	125.18	**+ ve**
C9	148.50	**+ ve**
C10	129.67	**0**
C11	119.82	**0**
C12	108.79	**– ve**
C13	149.87	**0**
C14	149.35	**0**
C15	106.75	**– ve**
C16	101.73	**– ve**

(**C**H_3 and **C**H = + ve ; **C**H_2 = – ve; **C**q = 0)

Table 3.1 Crystal Data, data collection and structure refinement parameters of compound 1.

Parameters	**1**
Empirical formula	$C_{18}H_{16}O_5$
Formula weight	312.31
Colour	Yellow Color
Habit	Block
Crystal Dimension (mm^3)	0.150 x 0.100 x 0.100
Crystal system	Monoclinic
Space group	$P2_1/c$
a (Å)	9.6821(5)
b (Å)	6.1513(3)
c (Å)	25.4709(14)
α (°)	90
β (°)	92.723(3)
γ (°)	90
Volume ($Å^3$)	1515.27(14)
Z	4
Temperature (K)	296(2)
D_C (Mg/m^3)	1.369
Absorption coefficient (mm^{-1})	0.097
$F(000)$	592
λ (Å)	0.71073
θ range (deg)	2.106 to 24.998
Scan type	ω, φ
Index ranges	-11<=h<=11, -7<=k<=7, -30<=l<=30
Reflections collected / unique obs.	17162 / 2682
R_{int}	0.0392
Refinement method	Full-matrix least-squares on F^2
Diffractometer	Bruker APEX2 X-ray diffractometer
Absorption correction	Multi-scan SADABS
Final *R* indices $R1/wR_2$ [$I>2\sigma(I)$]	0.0441/ 0.1064
$R1/wR_2$ (all data)	0.0864/ 0.1380
Goodness-of-fit on F^2	1.034
$\Delta\rho_{max/min}$, e $Å^{-3}$	0.163 and -0.167
Data / restraints / parameters	2682 / 0 / 211

Table 3.2 Selected bond lengths (Å) and angles (°) of compound 1.

Bond lengths (Å)		Bond angles (°)	
O(4)-C(16)	1.407(3)	C(16)-O(4)-C(14)	105.983(16)
O(4)-C(14)	1.376(3)	C(4')-O(5)-C(4)	117.62(18)
O(5)-C(4)	1.363(2)	C(16)-O(3)-C(13)	105.346(19)
O(5)-C(4')	1.414(3)	C(3')-O(2)-C(3)	116.25(18)
O(1)-C(7)	1.225(3)	O(3)-C(16)-O(4)	108.907(2)
O(3)-C(16)	1.41(3)	O(4)-C(14)-C(15)	127.877(2)
O(3)-C(13)	1.376(3)	O(4)-C(14)-C(13)	109.416(2)
O(2)-C(3)	1.366(2)	C(15)-C(14)-C(13)	122.706(2)
O(2)-C(3')	1.423(3)	C(10)-C(15)-C(14)	117.646(2)
C(15)-C(14)	1.361(3)	C(15)-C(10)-C(9)	118.4(2)
C(13)-C(14)	1.357(3)	C(11)-C(10)-C(15)	118.812(2)
C(15)-C(10)	1.398(3)	C(11)-C(10)-C(9)	122.78(2)
C(10)-C(9)	1.454(3)	C(10)-C(9)-C(8)	128.316(2)
C(11)-C(10)	1.383(3)	C(9)-C(8)-C(7)	121.753(2)
C(8)-C(9)	1.322(3)	O(1)-C(7)-C(8)	120.682(2)
C(8)-C(7)	1.460(3)	O(1)-C(7)-C(1)	118.886(2)
C(1)-C(7)	1.486(3)	C(1)-C(7)-C(8)	120.362(2)
C(6)-C(1)	1.381(3)	C(6)-C(1)-C(7)	123.88(2)
C(2)-C(1)	1.396(3)	C(2)-C(1)-C(7)	117.918(2)
C(5)-C(6)	1.386(3)	C(6)-C(1)-C(2)	118.12(2)
C(5)-C(4)	1.373(3)	C(5)-C(6)-C(1)	121.1(2)
C(3)-C(4)	1.402(3)	C(6)-C(5)-C(4)	120.112(2)
C(12)-C(11)	1.386(3)	O(5)-C(4)-C(5)	125.099(2)
C(12)-C(13)	1.358(3)	O(5)-C(4)-C(3)	115.259(19)
C(2)-C(3)	1.368(3)	C(5)-C(4)-C(3)	119.64(19)
		C(12)-C(11)-C(10)	122.356(2)
		C(11)-C(12)-C(13)	117.084(2)
		O(3)-C(13)-C(14)	110.31(2)
		O(3)-C(13)-C(12)	128.313(2)

C(12)-C(13)-C(14)	121.377(2)
C(1)-C(2)-C(3)	121.507(2)
O(2)-C(3)-C(4)	115.107(19)
O(2)-C(3)-C(2)	125.372(2)
C(2)-C(3)-C(4)	119.517(2)

Table 3.3 Torsion angles [°] of compound 1.

C(4')-O(5)-C(4)-C(5)	8.873(3)
C(4')-O(5)-C(4)-C(3)	-171.645(2)
C(3')-O(2)-C(3)-C(4)	170.864(2)
C(3')-O(2)-C(3)-C(2)	-9.869(3)
C(8)-C(9)-C(10)-C(15)	171.677(2)
C(8)-C(9)-C(10)-C(11)	-7.271(4)
C(10)-C(9)-C(8)-C(7)	-177.274(2)
O(1)-C(7)-C(8)-C(9)	-4.543(4)
C(9)-C(8)-C(7)-C(1)	172.384(2)
O(1)-C(7)-C(1)-C(6)	170.548(2)
O(1)-C(7)-C(1)-C(2)	-6.08(3)
C(6)-C(1)-C(7)-C(8)	-6.433(4)
C(2)-C(1)-C(7)-C(8)	176.939(2)

Table 3.4 Hydrogen bonds of compound 1.

D-H...A	d(D-H)	d(H...A)	d(D...A)	<(DHA)
C(15)-H(15)...O(1)#1	0.93	2.55	3.330(3)	141.5
C(3')-H(3')...O(2)#2	0.96	2.59	3.508(3)	159.6

Symmetry transformations used to generate equivalent atoms:

#1 -x+2,y-1/2,-z+3/2 #2 -x+3/2,-y+2,z+1/2